We are IntechOpen,
the world's leading publisher of
Open Access books
Built by scientists, for scientists

4,800
Open access books available

122,000
International authors and editors

135M
Downloads

Our authors are among the

154
Countries delivered to

TOP 1%
most cited scientists

12.2%
Contributors from top 500 universities

BOOK CITATION INDEX — CLARIVATE ANALYTICS — INDEXED

WEB OF SCIENCE™

Selection of our books indexed in the Book Citation Index
in Web of Science™ Core Collection (BKCI)

Interested in publishing with us?
Contact book.department@intechopen.com

Numbers displayed above are based on latest data collected.
For more information visit www.intechopen.com

EGS — Goodbye or Back to the Future

Reinhard Jung

Additional information is available at the end of the chapter

Abstract

The heat content of the crystalline basement is by far the biggest energy resource of the earth crust. First attempts to access this resource date back to the early 1970´th and more than a dozen research and industrial projects have been performed since than in various countries. But still the technique, known as HDR (Hot-Dry-Rock) or EGS (Enhanced-Geothermal-Systems) is not mature and the thermal power achieved so far does not meet economical standards. In addition further development is now hindered by the risk of induced earthquakes.

A critical review of results and observations shows that the main reason for the poor progress is the exploitation concept being applied in all major projects since the early 1980´th. Until than the basement had been regarded as a competent rock mass and the leading exploitation scheme was to connect two inclined boreholes by a number of parallel fractures created by hydraulic fracturing in short insulated borehole sections. Realizing that the basement contains open natural fractures even at great depth this multi-fracture-concept was abandoned and replaced by the EGS-concept. The intent of this concept was to enhance the permeability of the natural joint network by massive water injection in very long uncased borehole sections. The results of all major EGS-projects however shows that this is not happening but that generally one large wing-crack is created by the stimulation process regardless of the length of the test-interval. These wing-cracks require significantly bigger fluid volumes for the envisaged fracture-area, have a highly heterogeneous and anisotropic transmissibility and are a plausible explanation for the intense and strong induced seismicity as well as for the strong after-shocks observed at various EGS-locations. These findings suggest a return to the original multi-fracture concept with the only difference that the tensile fractures are to be replaced by the same number of wing-cracks. Directional drilling and packer technology improved significantly during the last three decades and multi-fracture concepts are applied with great success in unconventional gas reservoirs. Though the conditions and requirements in geothermal applications are more

demanding in various aspects it seems almost certain that geothermal multi-fracture-systems of this kind can be realized in the near future.

1. Introduction

Hydrothermal resources at relatively shallow depth used today for geothermal power production are just pinpoints on a map of global scale. By far the biggest resource of geothermal energy is the crystalline basement in regions with normal to slightly above normal temperature gradients. Although the crystalline basement is not completely impermeable due to the presence of open fissures, fractures, or faults its overall permeability is generally far too low to achieve and maintain production flow rates sufficient for geothermal power production. The majority of the crystalline basement may therefore be included among the "petrothermal resources". The basic concept of HDR- (Hot-Dry-Rock) or EGS-technology (Enhanced Geothermal Systems) thus consists of creating or enhancing large fracture surfaces in the crystalline basement in order to hydraulically connect two or several boreholes. During operation cold water injected in one of the boreholes heats up to rock temperature while circulating through the fracture system and is produced in the second well. To prevent boiling an overpressure is maintained in the geothermal loop. Steam for power generation is produced in a secondary loop.

Depending on drilling depth (usually > 3 km) and temperature (usually > 150 °C) a doublet system of commercial size will operate at flow rates between 50 and 100 L/s and produce an electric power of 3 - 10 MW_e. To ensure a service life of at least 25 years a separation distance of at least 0.5 to 2 km between the boreholes at depth and a total fracture surface area of 5 to 10 km^2 is required. The volume of rock to be accessed by the fracture system has to be in the order of 0.1 – 0.3 km^3. Due to the high flow velocities in the fractures especially near the injection and the production borehole the flow impedance of the fracture system (difference between inlet and outlet pressure devided by the outlet flow rate) is critical for the performance of the system. For energetic and economic reasons should not exceed 0.1 MPa s/L.

Basically two concepts had been designed and tested during the 40 years of HDR-research. In the beginning the crystalline basement at great depth had been regarded as an intact almost impermeable rock mass. It seemed therefore necessary to create artificial flow paths by means of hydraulic fracturing. The original concept (HDR-concept) [1-4] proposed by a group of the Los Alamos National Laboratory in the early 1970th consists of a doublet of deviated boreholes. The boreholes are drilled parallel to the azimuth of the least compressive principal stress and are connected by a set of large parallel fractures created during hydraulic fracturing tests in insolated borehole sections. These tensile fractures are oriented perpendicular to the least compressive principal stress.

The second concept (EGS-concept) promoted mainly by the Camborne School of Mines [5] and the University of Paris [6] is based on the observation of numerous natural fractures (joints and faults) even at great depth. The crystalline basement was therefore regarded as a broken material (discontinuum) and the idea was to shear and widen the natural fracture network by massive water injection in long uncased borehole sections. This process was named hydraulic

stimulation. The second borehole is then directionally drilled into the region of enhanced permeability. Since the stimulated region is elongated in the direction of the maximum horizontal stress, the boreholes are aligned in this direction which is 90 ° off the direction of the HDR-concept.
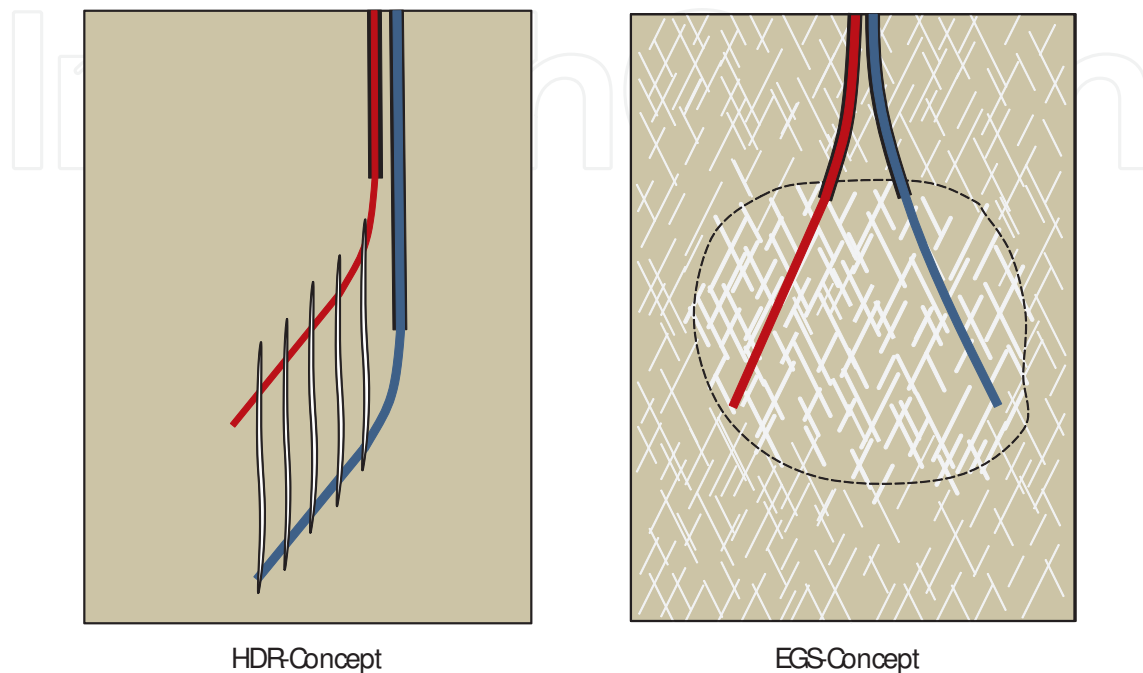

| HDR-Concept | EGS-Concept |

Figure 1. Basic concepts

Due to the enormous size of the created or enhanced fracture systems mainly water or brine without proppants were considered as frac-fluids since it seemed too costly or technically impossible to place proppant material over such large areas. All tests in the crystalline basement were accompanied by intense induced seismicity. Localizing and mapping the sources of induced seismicity thus became the most important tool for investigating the evolution of the fracture systems during water injection and most of the projects used this method to define the target for the second or third well. On the other hand induced seismicity has become a major obstacle for further development of the HDR- or EGS-technology since on some locations the population was shocked by events with magnitudes bigger than 3 [7].

The HDR-concept was followed only during the first years of development. Warned by the inability to create vertical fractures in the pioneering Los Alamos project and convinced by the arguments of the EGS-proponents that shearing of natural fractures is the predominant failure mechanism this concept was abandoned [8] and all projects after the 1980th followed the new EGS-concept. The rapid adoption of this concept was to a big part due to its technical simplicity. In particular, it required no high-temperature open hole packers, which created enormous technical problems in the Los-Alamos-Project. The change in the leading concept had severe consequences:

- Boreholes were no longer directional drilled parallel to the azimuth of the minimum horizontal stress but more or less parallel to the azimuth of the maximum horizontal stress.

- Very long almost vertical borehole sections containing hundreds of natural fractures were stimulated by injecting very large quantities of water.

- The development of high temperature packers was no longer important and was disregarded.

- Heat exchanging area as a measure for the service life of a HDR-system was replaced by accessible rock volume.

- Geometrical simple fracture mechanical models were replaced by geometrical complex fracture network models lacking fracture mechanical mechanisms.

It will be shown that mainly this change of concept is responsible for the poor progress of HDR-technology during the last 3 decades. The following chapters will critically review the results and observations of the major EGS-projects and proof that the basic mechanism controlling the stimulation process is not the shearing of the joint network but the formation of single large wing-cracks.

2. Characteristics of key projects

Nine research projects and 3 commercial HDR-projects have been performed since the beginning of Hot Dry Rock research at around 1970 [9]. The major projects are described briefly in the following paragraphs.

2.1. Los Alamos

This first HDR-project was located at Fenton Hill at the rim of a large caldera. HDR-Systems were established at two levels in a biotite-granodiorite body at around 2800 m depth (Fenton Hill I) and in a heterogeneous metamorphic complex below 3500 m (Fenton Hill II) [10]. Rock temperature was 190 °C at the upper level and above 230 °C at the lower level.

The main elements of the shallow system are two vertical fractures created by water-frac tests. The design of the deeper system was according to the HDR-concept as shown in Fig. 1. Since the Los Alamos team felt certain about the stress directions both boreholes were drilled and completed before stimulation. In the target zone the wells were directionally drilled with a dip of 60° and parallel to the azimuth of the minimum horizontal stress. The length of the uncased sections was 1000 m, their vertical distance 300 m. The deeper borehole reached a depth of 4400 m [3]. About a dozen hydraulic fracturing operations were conducted in various intervals of the deviated section of the deeper well (EE2). High temperature open hole packers, casing packers, and PBR (Polished Bore Receptacles) in combination with sanding-off the bottom part of the hole were used to insolate borehole sections of 20 to 150 m length within the 1000 m long open hole section [11,12]. Most of the tests showed a high frac-pressure of about 40 MPa (wellhead pressure) indicating a high value of the normal stress acting on the fracture (around

0.8 of the vertical stress). The most extensive hydraulic fracturing operation was conducted in the uppermost 20 m of the open hole at 3500 m depth by injecting 21,500 m³ of water at flow rates up to 130 L/s. From the spatial distribution of induced seismicity as shown in Fig. 2 it was concluded, that a volumetric structure of roughly 800 x 800 m with a thickness of 200 m was stimulated. The strike of this structure was perpendicular to the direction of the borehole azimuth as expected, but instead of being vertical it was dipping toward the East parallel to the borehole axis. A satisfactory connection between the boreholes could be achieved after sidetracking the upper well into the region of induced seismicity and after stimulating this new well section. A circulation test revealed a thermal power output of 10 MW at a production flow rate of 12 – 14 L/s. Fluid losses and flow impedance were 20–30 % and 2.1 MPa s/l respectively. The Fenton Hill test site was abandoned due to declining financial support.
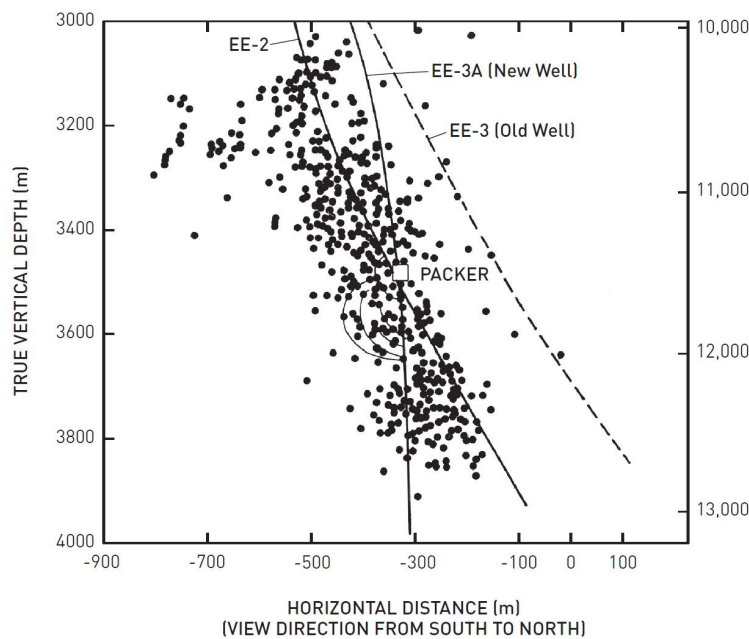

Figure 2. Hypocenters of seismic signals induced during the massive water frac-test in borehole EE1 at Fenton Hill (view is along the strike direction of the stimulated structure). EE-3A is the sidetrack of borehole EE-3, that was lend through the stimulated region. Note that the side track is not in the same plane as EE-2 but about 150 m in front of it. Re-production from [9].

2.2. Camborne

This first major project following the EGS-concept started in 1977 [5] and was operated by the Camborne School of Mines. The test site (Rosemanowes Quarry) is located near the centre of the Permian Carnmenellis granite pluton which is outcropping at the surface. Two orthogonal vertical joint sets were encountered at depth striking NNW-SSE and WSW-ENE. The stress conditions were strike slip with the maximum horizontal stress oriented NW-SE [13]. Two wells were drilled to 2000 m depth. Their arrangement is similar to the deep system in Fenton Hill but they deviate parallel to the direction of the maximum horizontal stress. Their vertical distance is about 300 m in the deviated part. Both boreholes had long open hole sections of 700

m and 360 m respectively. They were both drilled prior to stimulation. A hydraulic connection was achieved after a massive water injection in the lower well (26,000 m³) and a less massive stimulation in the upper well. The hydraulic connection however was poor and the fracture system extended during a long term circulation test with injection flow rates obviously too high for the system. A better connection was achieved after drilling a third well perpendicular to the strike of the fracture system and intersecting it some 300 m below the other two wells. Seismic activity recorded during the frac-tests (figure 3) showed that the activated fracture system had grown predominantly downward and was elongated in the direction parallel to the maximum horizontal stress [14]. The width of the seismic cloud (spatial distribution of the seismic sources) was less than 200 m. It showed an internal clustering of events along long vertical channels. A substantial thermal drawdown was observed during the first year of a circulation test indicating that the structure was much less "volumetric" than expected.
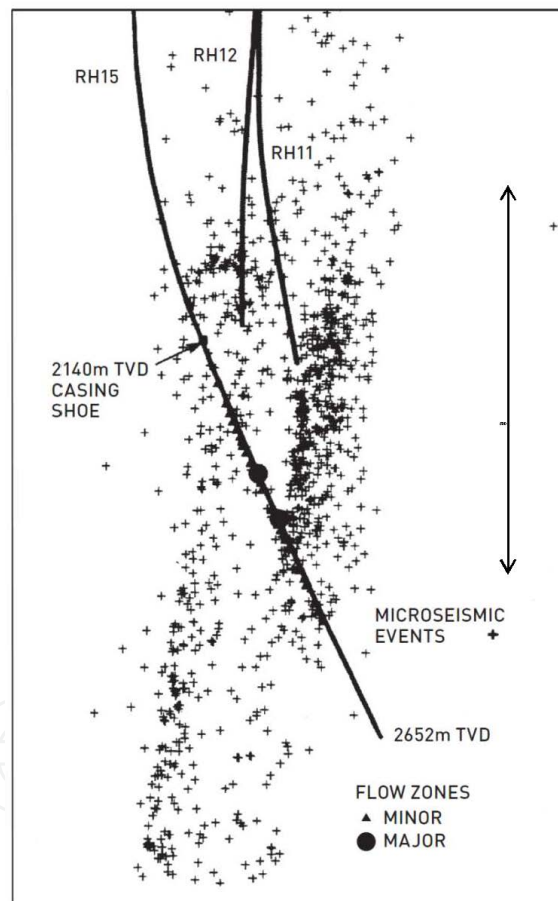

Figure 3. Front view of the seismic cloud of the EGS-system at Rosemanowes. Note the channel-like structures inside the seismic cloud. Re-production from [9]

2.3. Soultz-sous-Forêts

This project started in 1988 [15]. The site of Soultz is located in the central part of the Upper Rhine Valley 6 km east of the Western main fault. The top of the Granite is at 1400 m and holds

through down to the maximum depth of the boreholes (5 km). Typical for a rift setting is the high density of almost rift-parallel faults. Temperature anomalies at the site and in the region around Soultz are indications that some of the faults are permeable, transporting water from great depth into the Permian and Triassic cap rock. The joint systems are clustered with a high density of joints in fracture zones and a much lower density in competent rock [16]. Fracture zones and joints are mainly sub-vertical and striking 160°. The stress field is characterized by a low minimum horizontal stress ($\sigma_h \cong 0.54\,\sigma_V$) and a maximum horizontal stress almost equal to the vertical stress [17, 18]. It was supposed that there was a transition from normal faulting conditions in the top part to strike slip conditions below 3000 m. The direction of the maximum horizontal stress as determined from the orientation of drilling induced fractures and borehole break-outs is 170 °. Temperature reached 201 °C at 5000 m depth. Large scale in-situ permeability of the granite was determined to less than 35 μD. But some of the faults intersected by the boreholes had transmissibilities between 0.1 and 50 d m (darcy meter; 1 d m = 10-12 m³) demonstrating that much more than 90 % of the water in the granite is carried by a few highly permeable faults and not by the joint network [19, 20].

Two HDR-Systems were established in the depths levels 2800 – 3600 m [20] and 4400 m – 5000 m [21] respectively (figure 4). The design of both systems was according to the EGS-concept, but instead of drilling production and injection wells first and connecting them afterwards the first borehole was massively stimulated after completion and the next borehole directionally drilled into the target zone defined by the spatial distribution of induced seismicity. In this way a doublet system was established at the upper and a triplet system at the lower level. All boreholes drilled at Soultz had open hole sections of 500 – 750 m in the bottom part. These sections were stimulated by injecting large volumes of water (between 10,000 and 35,000 m³). Flow rates were comparatively low (35 – 55 L/s) and in some cases the tests were started at flow rates as low as 1 L/s in order to allow the pressure to spread out in the joint network thus stimulating as many joints as possible. Both in the upper and the lower system it was necessary to stimulate the second and (in case of the triplet) also the third well before a satisfactory connection was achieved. Borehole separation was 450 m in the doublet system and 600 m between the central injection hole and the two production holes in the triplet system.

Self propping of fractures was quite efficient and sustainable. Transmissibility of single fractures exceeded 1 d·m and was only slightly pressure dependent. Both fracture systems (upper and lower system) had open boundaries. Active pumping in the production wells was therefore introduced for the first time in an EGS-project in order to avoid fluid losses. Production flow rates reached 25 L/s in the production well of the upper system and more than 30 L/s for the two production boreholes (cumulated) of the lower system. Reinjection of the production flow in the central injection well of the lower system became a problem since induced seismicity started at an injection flow rate of about 20 L/s. In many aspects: depth, size, borehole distance, flow-impedance, circulation flow rates and fluid losses the two systems at Soultz mark the frontier of present HDR-technology. Part of this success however may be due to the favorable tectonic conditions in a rift setting and the results obtained so far are still insufficient for a commercial system.
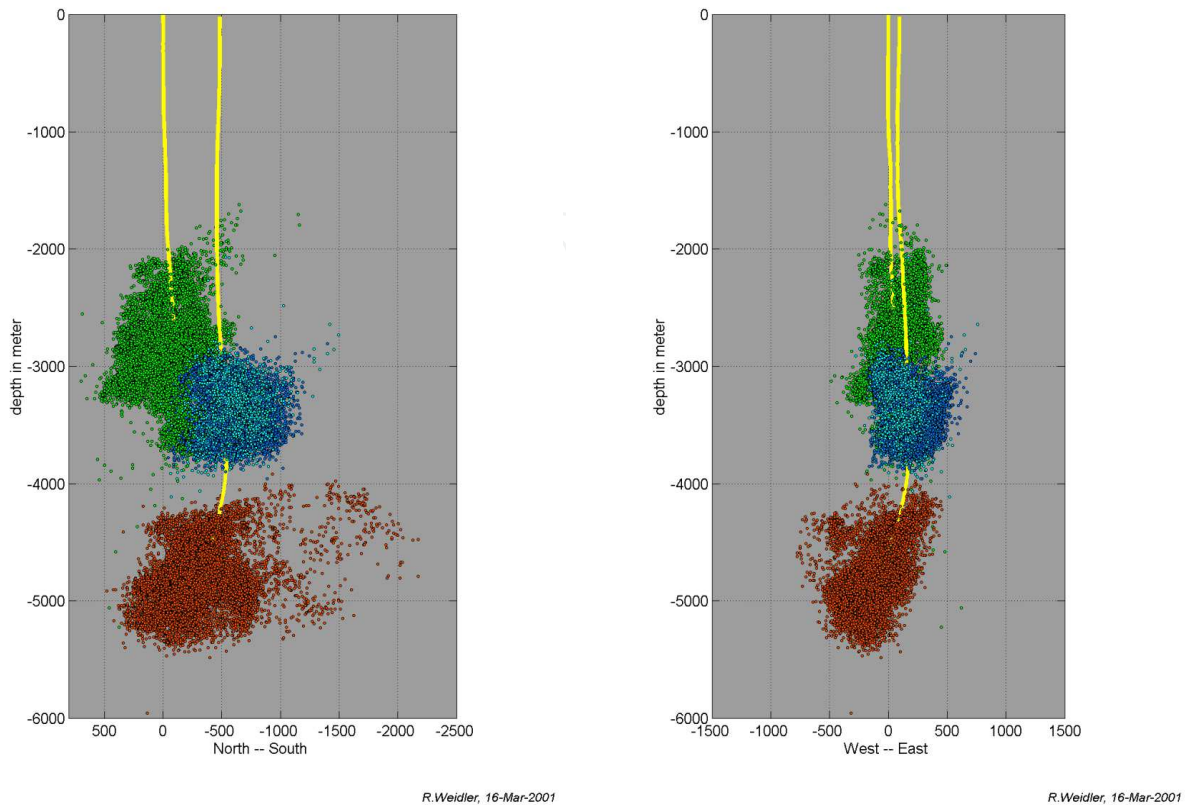
Figure 4. Seismic clouds of all stimulation tests of the upper EGS-system (Soultz I) and of the first stimulation test of the lower EGS-system (Soultz II) at Soultz [22]. General strike direction of the seismic clouds is NNW-SSE in both cases. The deeper well is GPK2, the other GPK1. The deep system was later intersected by two additional boreholes (GPK3 and GPK4) and enlarged during stimulation tests in these wells. Note the low seismic source density in the southern wing of the seismic cloud.

3. Observations and results of stimulation and circulation tests

Though the number of stimulation tests in EGS-projects is quite limited as compared to the millions of frac-tests in oil and gas reservoirs an attempt was made to find some general relationships between test-parameters and test-results. This was done with little hope since reliable data was sparse and test conditions very variable. The only constants for almost all tests were rock type (granite and granodiorite) and frac-fluid (water or brine with one exception) and the fact that all tests were done in uncased borehole sections. All other test parameters and conditions were quite variable (Tab. 1): Stress condition ranged from normal- to reverse faulting, length of frac-interval from 3 to 750 m, injected volume from 20 m³ to 35.000 m³, flow rates from 6 L/s to 200 L/s. Furthermore some tests were performed with constant flow rate, others with stepwise increased flow rates. Well trajectories were predominantly vertical to sub-vertical but some tests (Fenton Hill II and Camborne II) were performed in inclined borehole sections.

Project	Stress st.	Well	Frac-int.	Well Traj.	V_{IN}	Q_{IN}	P_{wc}	A	Cloud-Dip	Ref.
			[km]		[m³]	[L/s]	[MPa]	[km²]		
Falkenberg	normal	HB4a	0.25	vertical	25	3.5	2.2	0.014	60	[23]
Fenton H. I	normal		2.8	sub-vert.	587			0.15		[24]
Fenton H. I	normal		2.8	sub-vert.	761			0.16		[24]
Fenton H. I	normal		2.8	sub-vert.	5018			0.53		[24]
Fenton H. II	normal		3.7	55° II S_h	150			0.027		[24]
Fenton H. II	normal		3.7	55° II S_h	890			0.085		[24]
Fenton H. II	normal		3.7	55° II S_h	3183			0.27		[24]
Fenton H. II	normal		3.7	55° II S_h	3183			1		[24]
Fenton H. II	normal		3.7	55° II S_h	4702			1.1		[24]
Fenton H. II	normal	EE2	3.45-3.47	55° II S_h	22000	108	38	0.7	65	[8,12]
Camb. II	strike s.	RH12	1.74-2.12	60° II S_H	18500	20-90	14	0.6	sub-vert.	[25]
Camb. II	strike s.	RH15	2.1-2.25	60° II S_H	5700*	200	15	0.04	sub-vert.	[13]
Hijiori	normal	SKG-2	1.79-1.80	vertical	2000	17-100	15	0.15	60	[2,26,27]
Hijiori	normal	HDR-1	2.03-2.21	vertical	2100	17-67	26	0.25	60	[2,26]
Ogachi	(rever.)	OGC-1	1.00-1.01	vertical	10140	11	19	0.5	30	[2,28]
Ogachi	(rever.)	OGC-1	0.71-0.72	vertical	5440	8	22	0.3	sub-hor.	[2,28]
Soultz I	strike s.	GPK1	2.85-3.40	vertical	25300	0.2-36	9	1	sub-vert.	[20,29]
Soultz I	strike s.	GPK2	3.21-3.88	sub-vert.	28000	12-50	12	0.8	sub-vert.	[20]
Soultz II	strike s.	GPK2	4.40-5.00	sub-vert.	23400	30-50	14.5	3	sub-vert.	[22]
Cooper B.	reverse	Hab. 1	4.14-4.42	vertical	20000	14-26	60	3	sub-hor.	[9]
Basel	strike-s.	Basel 1	4.63-5.00	vertical	11650	0.2-55	30	0.9	sub-vert.	[30]

Table 1. Stimulation parameters and of major stimulation tests in HDR-projects, V_{IN}: injected volume, Q_{IN}: injection flow rate, p_{wc}: maximum well head pressure, A: area of the "seismic cloud"

3.1. General observations

General observations can be summarized as follows: All tests except a gel-test in the Camborne II system were accompanied by intense seismic activity. In all cases the seismic clouds were approximately 2-dimensional with a thickness in the range of the spatial resolution of the localization method. Some seismic clouds were twisted or bended or showed long tubular internal structures and straight boundaries. Width to length ratio measured along their main axis ranged generally from 0.3 to 3. The sparse seismic sources of the gel-frac were arranged tubularly. Some seismic clouds (Soultz II GPK2., Basel 1, and Fenton Hill II EE1) showed an alignment with well trajectories. Seismic clouds in strike-slip regions were vertical or sub-vertical with a general trend slightly off the direction of the maximum horizontal stress. For normal stress conditions (Hijiori, HDR-1 and Fenton Hill, EE2) the seismic clouds dipped 60° or 65° respectively toward the direction of the minimum horizontal stress. For reverse stress conditions (Cooper Basin and most likely Ogachi) the seismic clouds were horizontal or sub-horizontal. Seismic activity started generally far below the jacking pressure (pressure equal to the normal stress on the fracture) but the pressure always approached the at the end of the tests. In relation to depth the maximum injection pressure p_{wc} (measured at the well head) was comparatively low for vertical or sub-vertical fractures, higher for steeply dipping fractures and much higher for sub-horizontal fractures.

3.2. Size of the stimulated region

In contrary to the common praxis in EGS-literature of the last 2 decades but in accordance with an earlier study [24] not the volume but the area of the seismic cloud was taken as the measure for the size of the stimulated region. This was done because of the 2-dimensional nature of the seismic clouds and the strong influence of the location error on their thickness. This area, called seismic area in the following, was grossly determined by drawing an envelope around the projection of the seismic clouds on a plane parallel to its main orientation. Despite of the big variation in test and test-site conditions a clear correlation was found between seismic area and injected volume (figure 5a). 75% of the data points can well be fitted by a power law with exponent n = 0.6. Accordingly the ratio of injected volume and seismic area is fitted by a power law with exponent (1 – n) = 0.4 (figure 5b). Seismic area and the ratio of injected volume and seismic area did not correlate with flow rate or length of the frac-interval. These findings and the high coefficient of correlation of both parameters with injected volume allow establishing the following working hypotheses:

1. The stimulation process is mainly volume-controlled. This means, the majority of the injected volume is creating new fracture volume. Hydraulic diffusion (including fluid losses into the rock matrix) is not essential. Fluid efficiency η (ratio of created fracture volume and injected volume) is high (at least higher than 0.5).

2. The number of fractures created or stimulated in the frac-interval is close to "1" regardless of the length of the frac-interval.

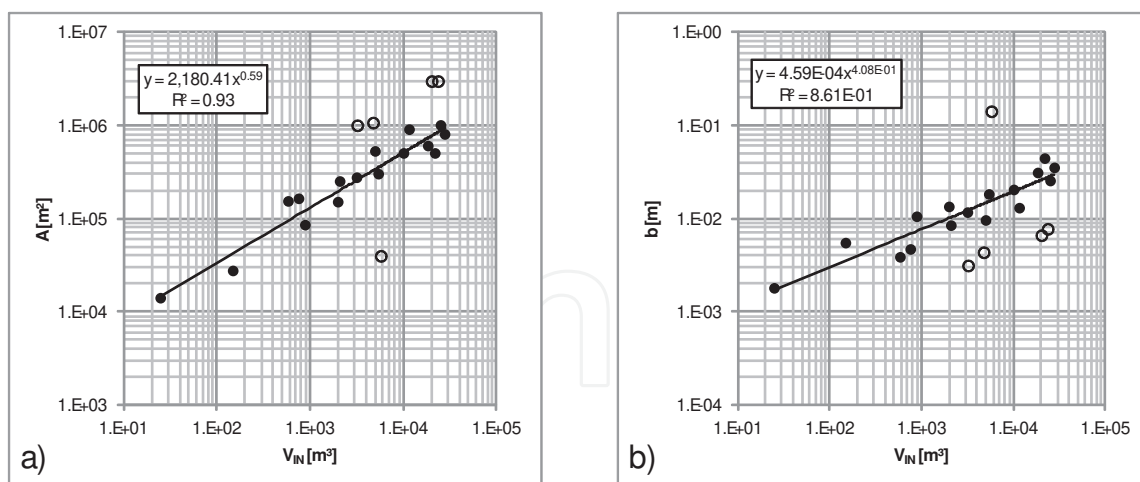3. Static fracture models should apply; friction pressure losses in the fractures are negligible.

Figure 5. Results of the stimulation tests: a) Area of the seismic clouds vs. injected volume, b) ratio of seismic area and injected volume vs. injected volume. Fitting lines and coefficients of determination are for the solid data points.

3.3. Characteristics and internal structure of the stimulated region

Some of the seismic clouds showed long channel-like internal features. In the Soultz I system a first channel started to grow from the main outlet in the top part of the open hole section of

the first well (GPK1) and propagated sub-vertically downward (figure 6). At the end of stimulation it reached a length of about 700 m. Seismicity was spreading predominantly to one side of this channel during migration. In the final test period several other channels developed starting from almost the same region as the first but with different dip (figure 6). Views along some of these channels indicate that the main structure created by the stimulation process was a large wing crack with a central shear zone and the typical bended wings (figure 7).
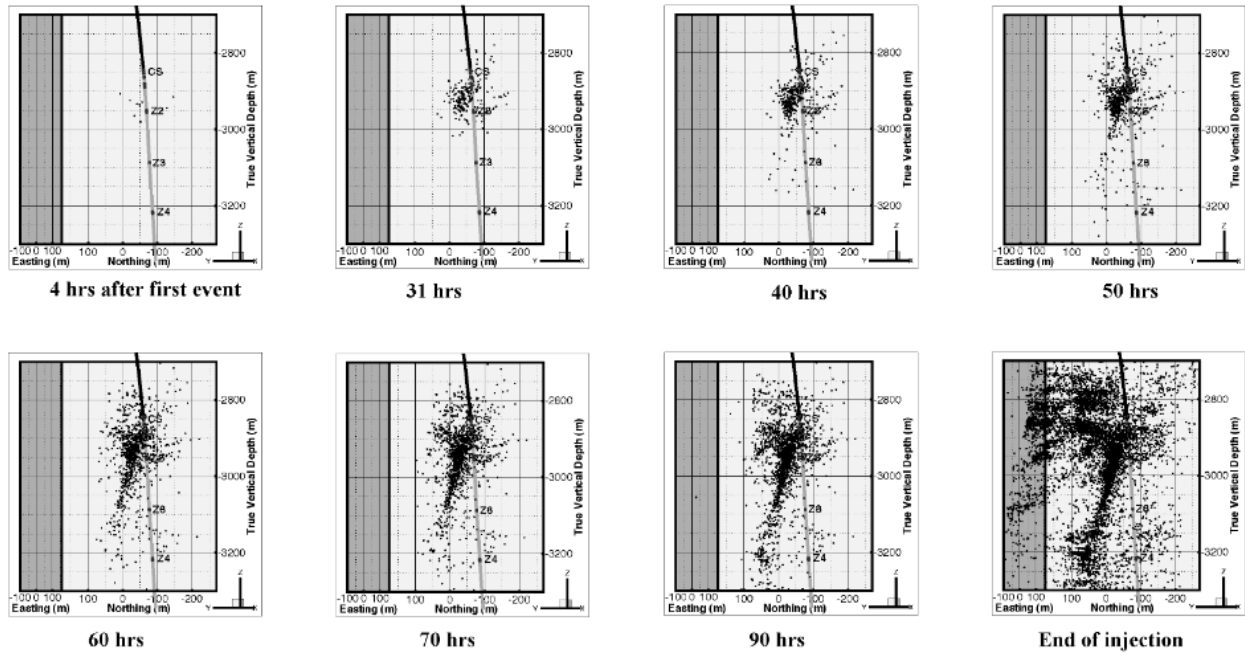
Figure 6. Evolution of the seismic cloud during the first stimulation test in the Soultz I system (front view) [31].
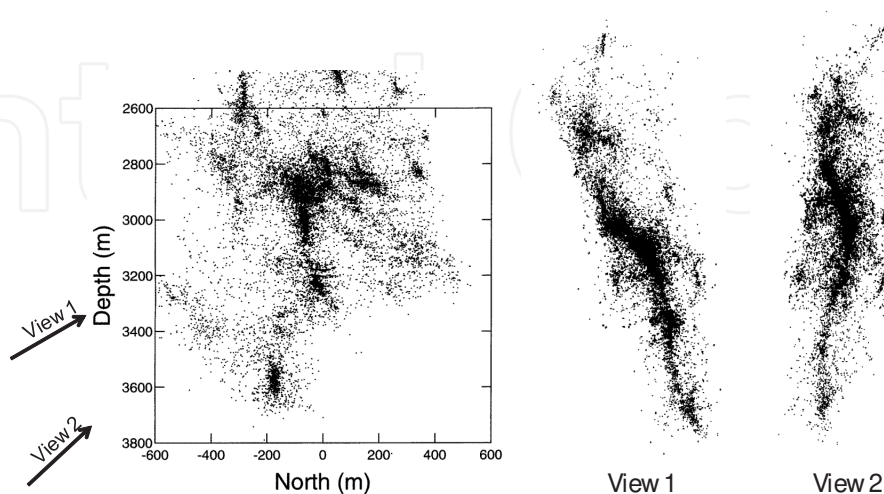

Figure 7. Seismic cloud of all located events of the first stimulation test in the Soultz I system (well GPK1). Left: front view, middle and right: views along indicated directions [32].

3.4. Number of stimulated fractures

Direct information on the number of conductive fractures was obtained by flow and temperature logging during stimulation and post-stimulation injection or production tests. In no case was the number of hydraulically significant fractures bigger than 4 and often they were in close vicinity to each other. An example from a well in the Soultz I system as shown in figure 8 demonstrates that even these small numbers should only be regarded as an upper limit [32]. The 750 m long uncased section of this well contained one significant fault with a transmissibility of 0.1 d m at 3500 m depth prior to stimulation. This fault consumed more than 90% of the injected fluid during pre-stimulation hydraulic tests. The contribution of the several hundreds of joints, a number of fracture zones and additional faults, as well as the numerous drilling induced fractures encountered by ultrasonic borehole-televiewer measurements was insignificant. During stimulation a group of drilling induced en-echelon fractures in the uppermost open hole section opened in the early test-phase and remained the dominant hydraulic feature throughout the test absorbing about 2/3 of the injected flow rate. The remaining third was absorbed by the fault at 3500 m and by 3 other fractures. A redistribution of the flow fraction of these three fractures between stimulation and production proofed that they were merely low impedance connections to the main fracture originating in the uppermost part of the open hole section (figure 8).
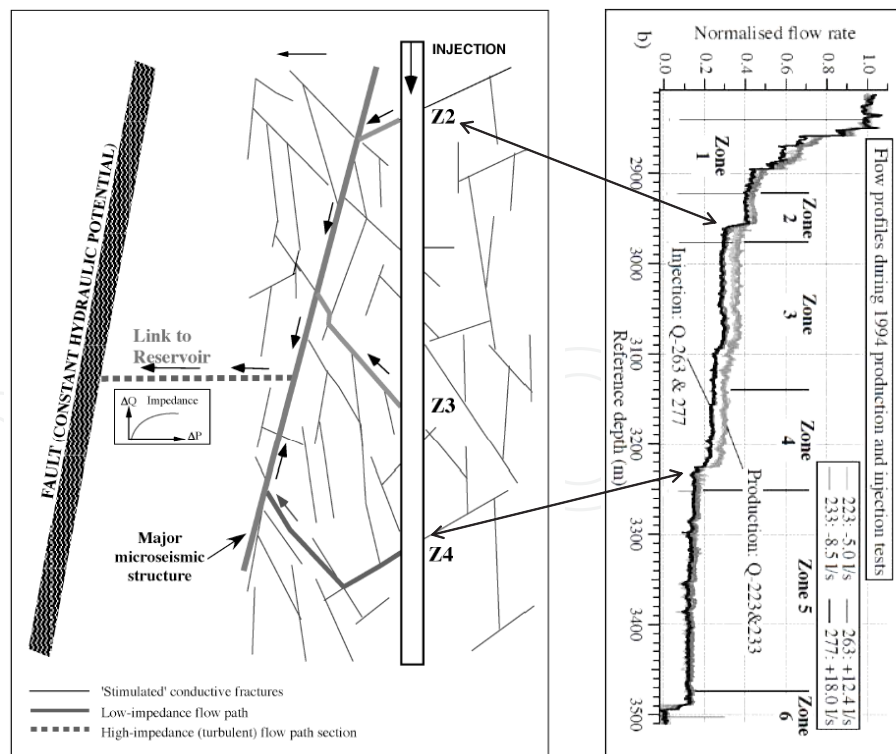

Figure 8. Right: Spinner flow logs recorded during the main stimulation test and during a post-stimulation production test in well GPK1 (Soultz I system). Left: model illustrating that fractures Z1, Z2, and Z3 are low impedance flow paths connection the well to the main fracture Z1 [31].

3.5. Aperture of stimulated fractures

Information on the aperture of the stimulated fractures can be obtained from tracer tests performed during circulation. The tracer response curves of EGS-systems found in reports and publications were of surprisingly uniform shape (figure 9). All had a steeply rising tracer concentration after tracer break-through, a single maximum and a monotonously declining tracer concentration afterwards. Some showed minor inflections in the tail that were interpreted by some authors as tracer arrivals from multiple flow paths but as an effect of tracer re-injection by others. None of the curves showed clear indications of multiple fracture flow.
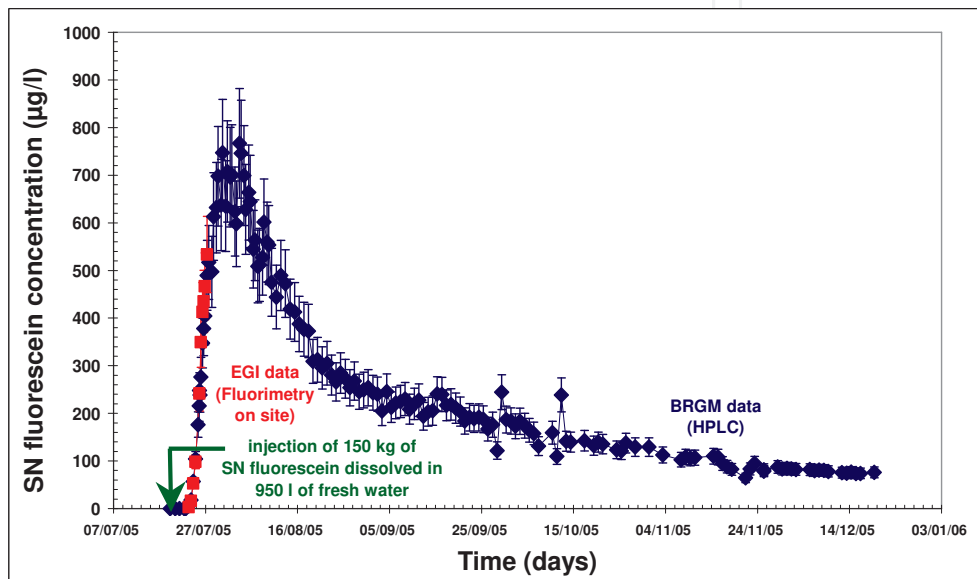

Figure 9. Tracer response curve recorded during a long-term circulation test in the Soultz II system. Source: [33].

For these reasons and in order get comparable results it seemed reasonable to use the same simple proxy model, namely that of a doublet in an infinite fracture of uniform aperture for evaluation. The tracer break-through volume for this model is given by:

$$V_b = \frac{\pi b_T \cdot a_G^2}{3} \tag{1}$$

With b_T: aperture of the fracture and a_G: geometrical inlet to outlet distance. The values of b_T determined with this equation are listed in Table 2 and plotted in figure 10. For comparison the values of b given by the ratio of seismic area and injected volume and the corresponding fit-line are included. In 3 cases (Fenton Hill I & II and Camborne II) is the aperture determined from the tracer break-through volume by a factor of 5 to 10 smaller than the aperture given by the ratio of injected volume and seismic area. In other 3 cases (Soultz I, Hijiori and Ogachi) both aperture values agree quite well. For Soultz II the aperture from the tracer break-through volume is consistent with the data from Soultz I, Hijiori and Ogachi though the ratio of injected volume and seismic area is comparatively low. The majority of the aperture values are in the

range of centimeters. For comparison: (hypothetical) tensile fractures with a fracture area of 1 km² would have an average aperture of about 1 mm.
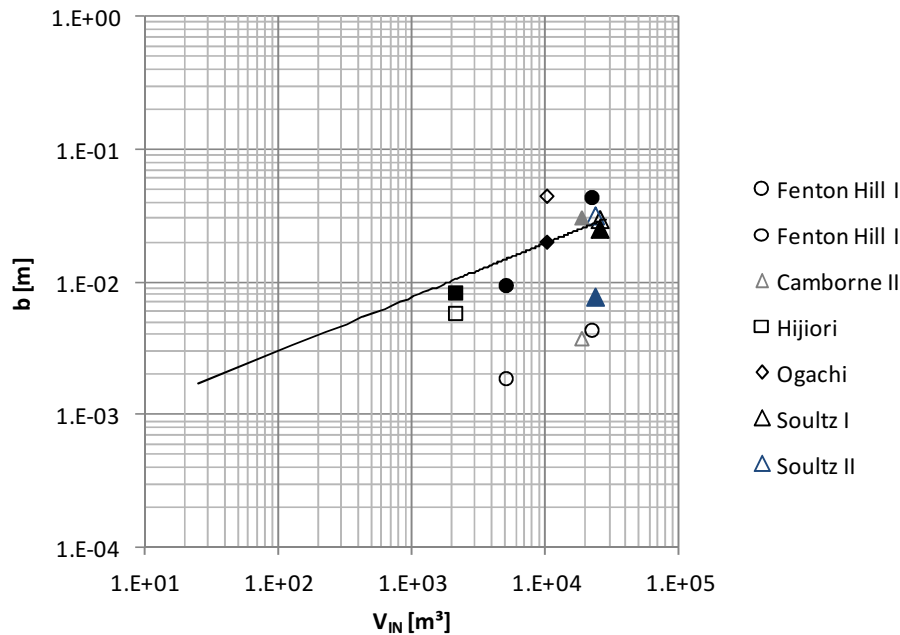

Figure 10. Fracture apertures determined from tracer break-through volumes (open symbols) and given by the ratio of injected volume and seismic area of the stimulation tests (filled symbols). Fitting line is identical with the fitting line of figure 5b.

3.6. Heat exchanging area

The observation of the thermal draw down is probably the most sensitive method to distinguish single fracture flow from multi-fracture or volumetric flow. Already two (thermally independent) fractures instead of one extent the time scale for the thermal draw-down by the square-root of two. Volumetric flow is indicated when the production flow is constant over a prolonged time period. Unfortunately data for only two cases, Camborne II and Hijiori was available. Both thermal draw down curves could well be fitted by using an analytical model and reasonable thermo-physical values for the fluid and rock. The model calculates the evolution of the production temperature for a doublet in an infinite fracture of uniform transmissibility with transient conductive heat flow from the rock matrix toward the fracture (figure 11). The inlet-outlet distance of 260 m determined by using this model agrees quite well with the geometrical inlet-outlet distance of the Camborne II system (Table 2). For two fractures this distance would reduce to 190 m, which is hardly compatible with the geometrical configuration. For Hijiori the inlet-outlet distance obtained by the model is already for one fracture smaller than the geometrical distance. Two fractures would make this discrepancy even bigger. The thermal draw down curve of a porous layer with a thickness of 10 m instead of a discrete fracture would have a thermal break through-time (end time of constant production temperature) of about 1 year for Camborne (figure 11). The observed thermal break-

through time is by at least a factor of 10 lower. This means a layer compatible with the thermal draw-down of Camborne II could have a maximum thickness of 1 m. The long term thermal response of such a layer is indistinguishable from that of a discrete fracture. Summarizing one can conclude that the observed thermal draw down curves give no reason to introduce more than one fracture or a porous layer (volumetric fracture system) instead of a discrete fracture as the main flow path between injection and production well.
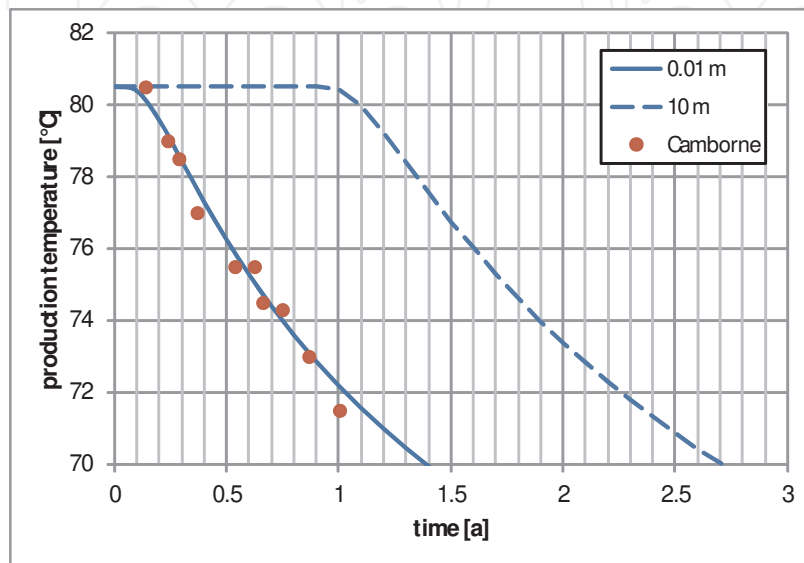

Figure 11. Evolution of the temperature draw-down in the production well of the Camborne II system (red dots from [34]) and fit-curve calculated for a doublet in an infinite fracture (solid blue line) and for a doublet in a porous layer with thickness 10 m (dashed line) for well distance: $a_H = 263$ m, flow rate: $Q = 15$ L/s, injection temperature: $T_{in} = 20$ °C, $T_0 = 80.5$ °C.

3.7. Hydraulic properties

The inter-well transmissibility of the fractures was determined from the flow impedance "I" by using the model of a doublet in an infinite fracture of homogeneous and isotropic transmissibility imbedded in an impermeable matrix. For this model the transmissibility is approximately given by the following formula:

$$T_f = \frac{2\mu}{I} \; \left[m^3\right] \tag{2}$$

The values calculated with Eq. 2 are listed in Tab. 2. The transmissibility of the fractures of the Camborne II and the Soultz I & II systems exceeds 1 d·m, a value which is rarely achieved with conventional propped fractures. The fractures of the other systems are in the range of 0.1 d·m or lower. The "hydraulic aperture" b_H corresponding to these transmissibility values can be calculated by:

$$b_H = \sqrt[3]{12 T_f} \tag{3}$$

This formula is for smooth fracture surfaces and was experimentally confirmed for fractures in rock but with coefficients slightly higher than 12. The hydraulic apertures calculated with this formula are by about a factor of 10 to 100 lower than the apertures derived from the tracer break-through volume (Tab. 2). This in turn means that one should expect fracture transmissibilities between 500 d·m and 7 Mio. d·m from the apertures of the tracer tests. This stupendous discrepancy can not be explained by turbulence or viscosity effects. It is also unlikely that asperities or particles are plugging the fractures to such a degree that only a small fraction of the fractures is open for the flow. In this case the tracer break-through volume would also be reduced to a high degree. The most plausible explanation is that the fractures consist of a series of wide open and very narrow fracture elements. In this case the average aperture is mainly determined by the wide fracture elements whereas the transmissibility is mainly determined by the narrow fracture elements. This kind of arrangement can neither be explained by tensile fracture propagation nor by the shearing of existing fractures or faults.

Project	a_G	T_0	Q_{EX}	I	μ	T	b_f	V_b	b_T	a_H	References
	[m]	[°C]	[L/s]	[MPa·s/L]	[Pa·s]	[d·m]	[m]	[m³]	[m]	[m]	
Fenton Hill I	230	190	6	1.6	1.5E-04	.19	1.3E-04	100	1.8E-03	-	[9]
Fenton Hill II	150	230	6	2.1	1.3E-04	0.12	1.2E-04	100	4.2E-03	-	[8] [3]
Camborne II	250	80	15	0.6	3.6E-04	1.20	2.5E-04	240	3.6E-03	263	[13]
Hijiori	90	250	4	0.6	1.2E-05	0.04	7.9E-05	90	1.1E-02	65	[35-38]
Ogachi	80	240	1.7	8	1.2E-04	0.03	7.2E-05	289	4.3E-02	-	[39]
Soultz I	450	170	25	0.23	1.6E-04	1.39	2.6E-04	6000	2.9E-02	-	[20]
Soultz II	600	200	12	0.25	1.4E-04	1.1	2.4E-04	11500	3.1E-02	-	[34]

Table 2. Operation parameters and results of circulation tests in major HDR-systems, a_G: geometrical distance between inlet and outlet, T_0: rock temperature, Q_{EX}: production flow rate, I: impedance (ratio of pressure difference between inlet and outlet and production flow rate), μ: viscosity of produced water; T: transmissibility, b_H: hydraulic aperture, V_b: tracer break-through volume, b_T: aperture calculated from tracer break-through volume, a_H: inlet to outlet distance calculated from observed thermal draw-down.

Well test analysis of post-stimulation injection or production tests point into the same direction. All post-stimulation hydraulic tests in Soultz and in Basel showed very long fracture linear or bilinear flow periods often persisting over 10 hours or more. Such long periods need a very long start line for the flow. In cases where several hundred Meter long axial fractures are present (Soultz II well GPK4 and probably Basel) these long starting lines may be identical with the trace of these fractures along the borehole wall. In other cases they are most likely identical with the long channel-like features of the seismic clouds. Theses channels play most likely a dominant role for the flow distribution in the stimulated fractures. Channels may also exist on the scale of joints and may result in a highly anisotropic transmissibility of the large scale fracture.

4. Interpretation and discussion

It is obvious that the actual EGS-concept is inconsistent with almost all observations and results described in the last chapter. The main reason for this inconsistency is most likely the wrong model for the granite underlying this concept. It´s basic assumption is that the granite due to the presence of joints has to be considered as a discontinuum (figure 12) and can therefore be regarded a as coulomb-material. Accordingly the coulomb friction failure criterion is the obvious choice for the stimulation process. A more realistic model (figure 12) however considers the granite as a continuum on the scale of joints and as a discontinuum on the scale of faults or fracture zones [41, 42].
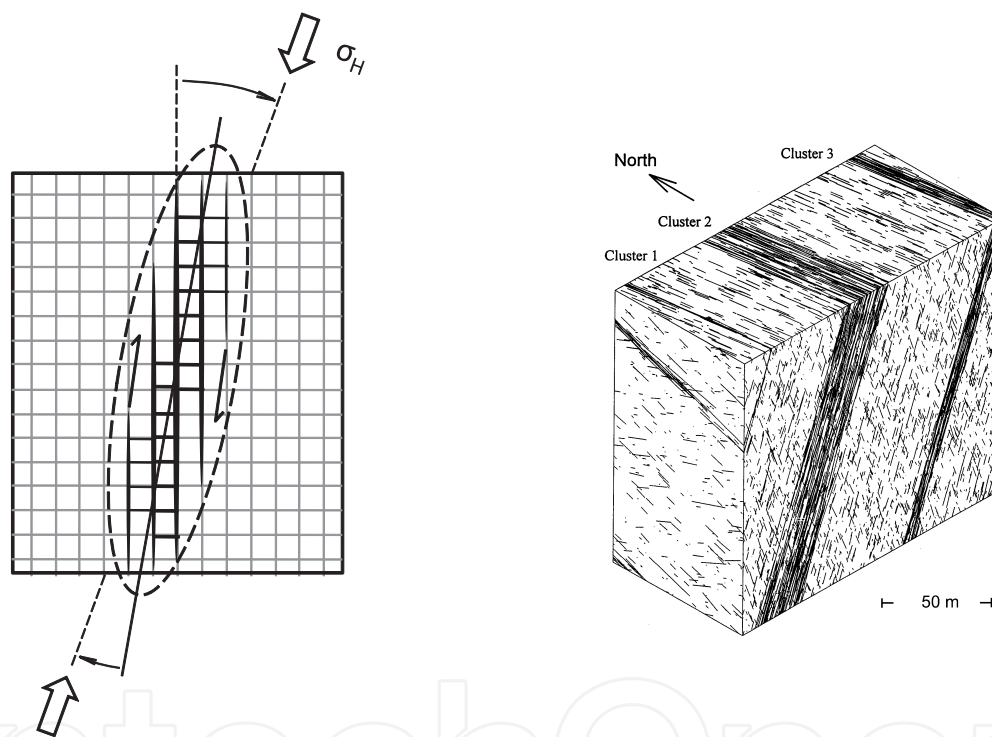

Figure 12. Conceptual models for the granite. Left: granite as a discontinuum on the scale of joints [13], right: granite as a discontinuum on the scale of faults or fracture zones and as a continuum on the scale of joints [40, 41].

The Coulomb failure criterion is therefore applicable only on the scale of faults or fracture zones whereas on the scale of joints hydraulic stimulation needs a failure mechanism that includes the formation of new fracture surface like the classical hydraulic fracturing models. Tensile fracture models are however unable to explain the onset of the failure process at a pressure far below the minimum principal stress. Furthermore they are hardly consistent with the intense seismicity and the source mechanism of the seismic events. For these reasons a new model is required that combines tensile fracture propagation with the shearing of natural discontinuities. The most obvious choice is the wing-crack model (figure 13).
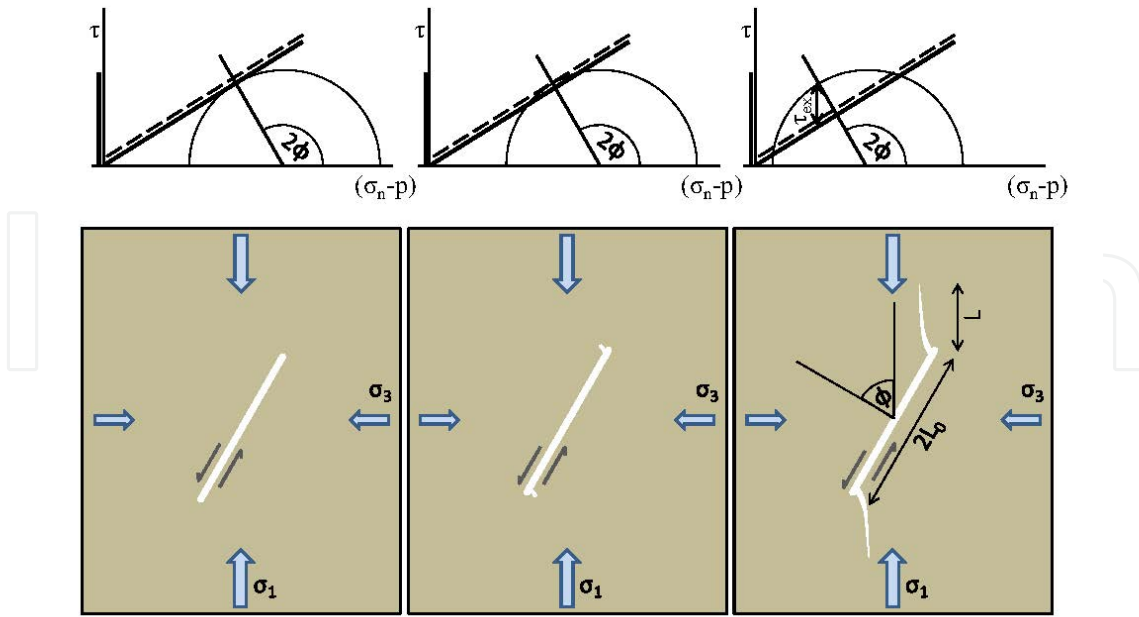
Figure 13. Wing-crack model, left: onset of shearing, middle: wing initiation, right: wing propagation.

The formation of wing-cracks is one of the micro-mechanisms discussed in material science to explain the inelastic behavior and failure of brittle material under compression. The basic observation is that fractures of finite length failing in shear will not propagate along their own plane but will form tensile wing-fractures (figure 13). Referring to results of [42] Lehner & Kachanow [43] stated that the wings start to grow at an angle of 70° to the plane of the initial shear fracture and gradually turn into the direction of the maximum principal stress. Intro-ducing the parameter τ_{ex} which is the part of the shear stress exceeding the Coulomb friction failure line (figure 13) the criterion for the initiation of the wings can be written as [42]:

$$\tau_{ex} = \frac{\sqrt{3}K_{IC}}{2\sqrt{\pi L_0}} \tag{4}$$

With $\tau_{ex} = \tau - \mu(\sigma_n - p)$, τ: shear stress on the fracture, σ_n: normal stress on the wings, p: fluid pressure in the wings, K_{IC}: fracture toughness of the rock, L_0: half length of the initial fracture (figure 13). Inserting typical values for the fracture toughness of granite $K_{IC} = 1.5$ MPa m$^{1/2}$ and for the joint half length $L_0 = 5$ m one gets $\tau_{ex} = 0.33$ MPa. This low value indicates that joints being sheared will inevitably develop wings.

In the simplest approximation of long straight wings parallel to the axis of the maximum principal stress propagation of the wings of a stress driven fracture is governed by the following equation [24]:

$$\sqrt{\frac{L}{L_0}} = \frac{K_{IC}}{2(\sigma_3 - p)\sqrt{\pi L_0}} + \sqrt{\left(\frac{K_{IC}}{2(\sigma_3 - p)\sqrt{\pi L_0}}\right)^2 + \frac{2\tau_{ex}\cos\phi}{\pi(\sigma_3 - p)}} \tag{5}$$

With L: length of the wings, σ_1, σ_3: maximum and minimum principal stress respectively, p: fluid pressure in the wing-crack, Φ: angle between the normal of the joint and the maximum principal stress. For wing-cracks of the scale of joints or bigger the terms containing fracture toughness K_{IC} can be neglected and the equation reduces to:

$$\frac{L}{L_0} = \frac{2\tau_{ex}\cos\phi}{\pi(\sigma_3 - p)} \tag{6}$$

This formula shows that wing propagation is stable as long as the fluid pressure is smaller than the minimum principal stress and that the wing length can become long in comparison to L_0 only when the fluid pressure approaches σ_3. This means, in competent granite (with a low density of joints) large scale wings (in relation to the size of the joints) can only develop at a pressure close to the frac-extension pressure of conventional tensile fractures. In fracture zones where the joint density is high the situation is different (figure 14). Here the wings of the joint being sheared first may connect to the next pair of joints soon after their initiation. The fluid-pressure required for this is presumably not much higher than the pressure for wing initiation. When this pressure is maintained a through-going series of joints and wing-cracks can develop. This series is acting as one large scale shear fracture. Correspondingly much larger wings can emerge from the end of this series than from the ends of a single joint when exposed to the same pressure.
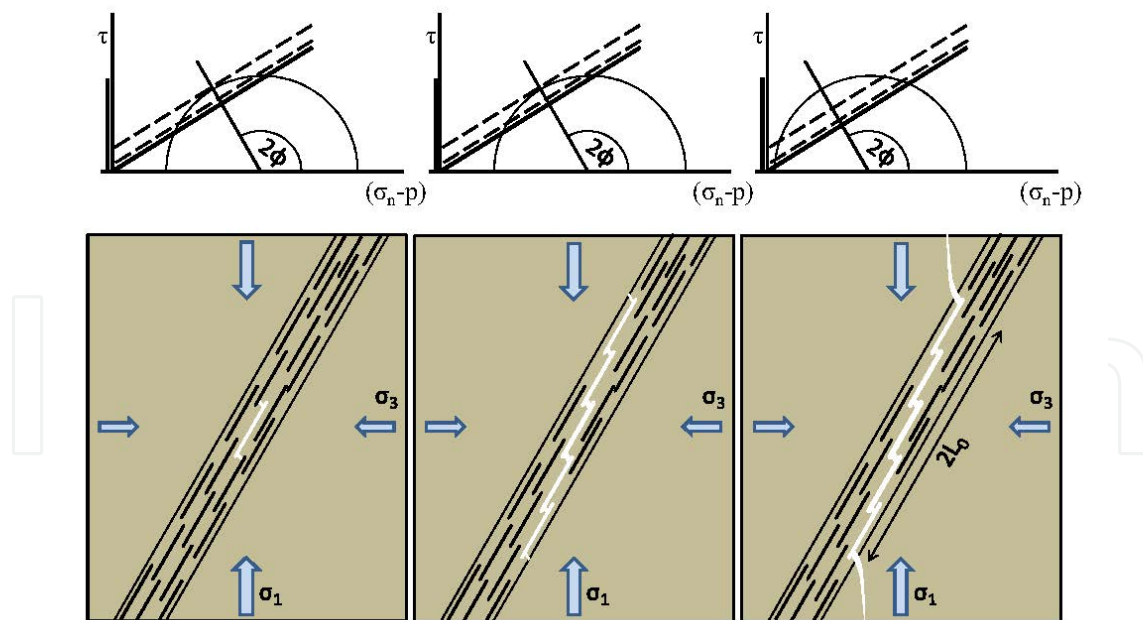

Figure 14. Wing-crack mechanism in a fracture zone, left: wings of the first sheared joint connect to the next pair of joints, middle: chain of wing-cracks reach the boundaries of the fracture zone, right: large scale wings emerge from the boundary of the fracture zone.

Before the wings become very long they will probably grow in height, i.e. in the direction perpendicular to the 2-D wing-crack model of figure 14. This can happen at any fluid-pressure higher than the pressure given by equation 4. This is a plausible explanation for the evolution of the channel-like features in the seismic clouds preceding their lateral propagation. It seems that stimulating at low flow rates as in Ogachi and in the starting periods of Basel and Soultz accentuate the formation of these channels but channeling was indicated also on other sites. For normal and reverse stress conditions these channels were predominantly horizontal or sub-horizontal (Fenton Hill, Hijiori, Ogachi, and Cooper Basin). For strike slip conditions they were pre-dominantly vertical or sub-vertical (Soultz, Basel, Camborne). In the Camborne system extremely long vertical channels developed during a long term circulation test. This demonstrates that the wing-crack mechanism may lead to uncontrolled large scale fracture growth during the operation of the EGS-Systems at a fluid pressure significantly lower than the minimum principal stress.

Neglecting fracture toughness the normalized shear displacement at the root of the wings is approximately given by:

$$\frac{U}{L_0} = \frac{4 \cdot \tau_{ex}}{E'}$$ (7)

With E': Young´s modulus for plane strain conditions. This equation is a good approximation of a formula given in [43] for the straight wing model. The normalized aperture of the wings at their root is given by:

$$\frac{b}{L_0} = \frac{4\tau_{ex}cos\phi}{E'}$$ (8)

These formulas were applied to the stimulated fracture in Basel, whose seismic cloud showed a remarkably clear wing-crack shape (figure 15) after processing source location data with the so called "collapsing method" [44].

The results of the wing-crack model agree quite well with the observations when an angle of Φ = 80° is assumed. This direction is within the uncertainty-limits of the stress data [30]. The calculated ratio of $L/L_0 \approx 2$ agrees quite well with the observed data (figures 15, 16). Similarly yields the wing-crack model the same large aperture values as derived from the tracer tests and from the ratio of injected volume and seismic area. For comparison: Static tensile fracture models like the 2-D Griffith fracture would yield average apertures of about 1 mm. One of the most striking results is the very high displacement of 100 mm at the root of the wings (for Φ = 80°). This easily explains the high number of seismic events and the occurrence of high magnitudes in the central part of the seismic cloud of Basel. Interestingly the wings showed up only during the shut-in and flow-back period though they had presumably been formed much earlier. This and the fault plane solutions of the post-fracturing events [30] indicate that the seismic signals of the wings were induced not by forward-sliding but by back-sliding. This behavior can hardly be explained by shearing of a natural fault but is easily explained with the wing-crack model. The low density of seismic sources of the wings as observed in Basel is

not surprising. Since they are tensile fractures they may only show up where they intersect prominent natural discontinuities and cause them to shear.
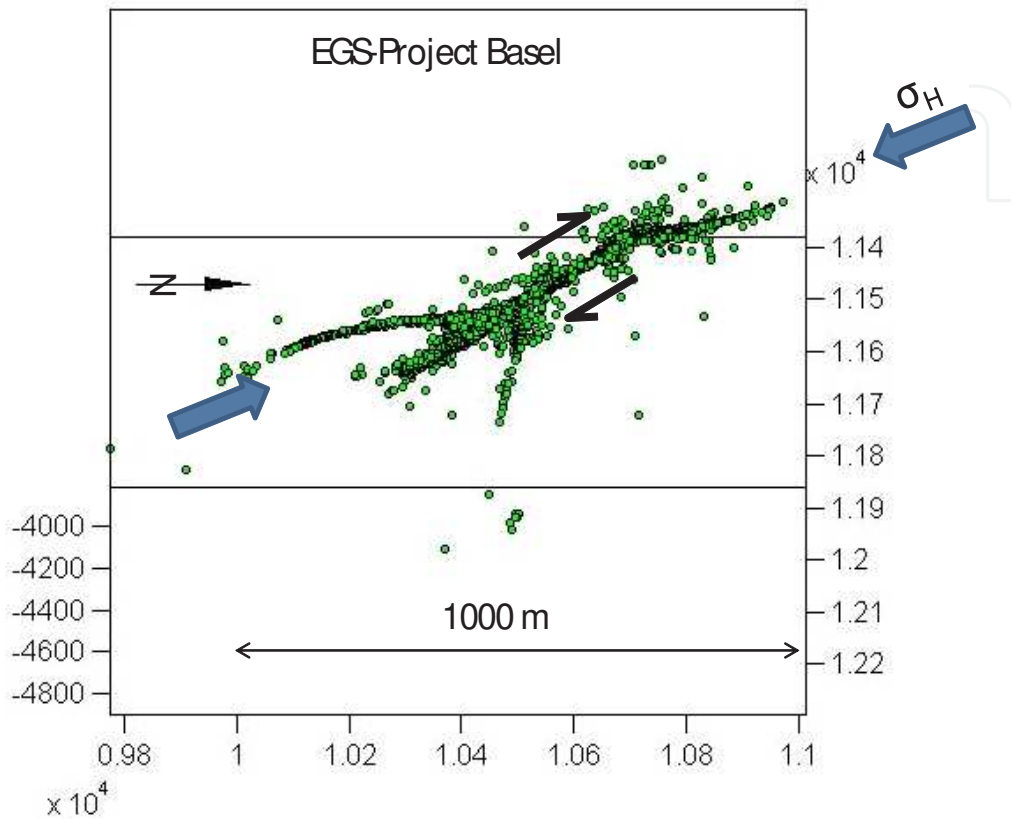

Figure 15. Processed (collapsed) seismic cloud of the stimulation test in Basel, view about 10° from vertical toward W, blue arrows: direction of the maximum horizontal stress, collapsing performed by Q-Con GmbH [44], stress direction [30].

Generally the large scale wing-crack model delivers a plausible explanations for almost all observations described in the previous chapters in particular for: the onset of fracture propagation at a fluid pressure much lower than the minimum principal stress, the high intensity and mechanism of induced seismicity, the occurrence of channel-like features in the seismic clouds, the long lasting fracture linear or bilinear flow periods during post-stimulation well tests, the occurrence of high magnitude after-shocks, the large fracture apertures derived from tracer break-through volumes and from the ratio of fracture area and injected volume. It also explains the striking discrepancy between the only moderate fracture transmissibility and the large apertures. It is clear that a more rigorous study requires 3-D-wing-crack models since the 2-D-model neglects the vertical stress gradients and it may be due to these stress gradients that some of the seismic clouds showed twisted wings.
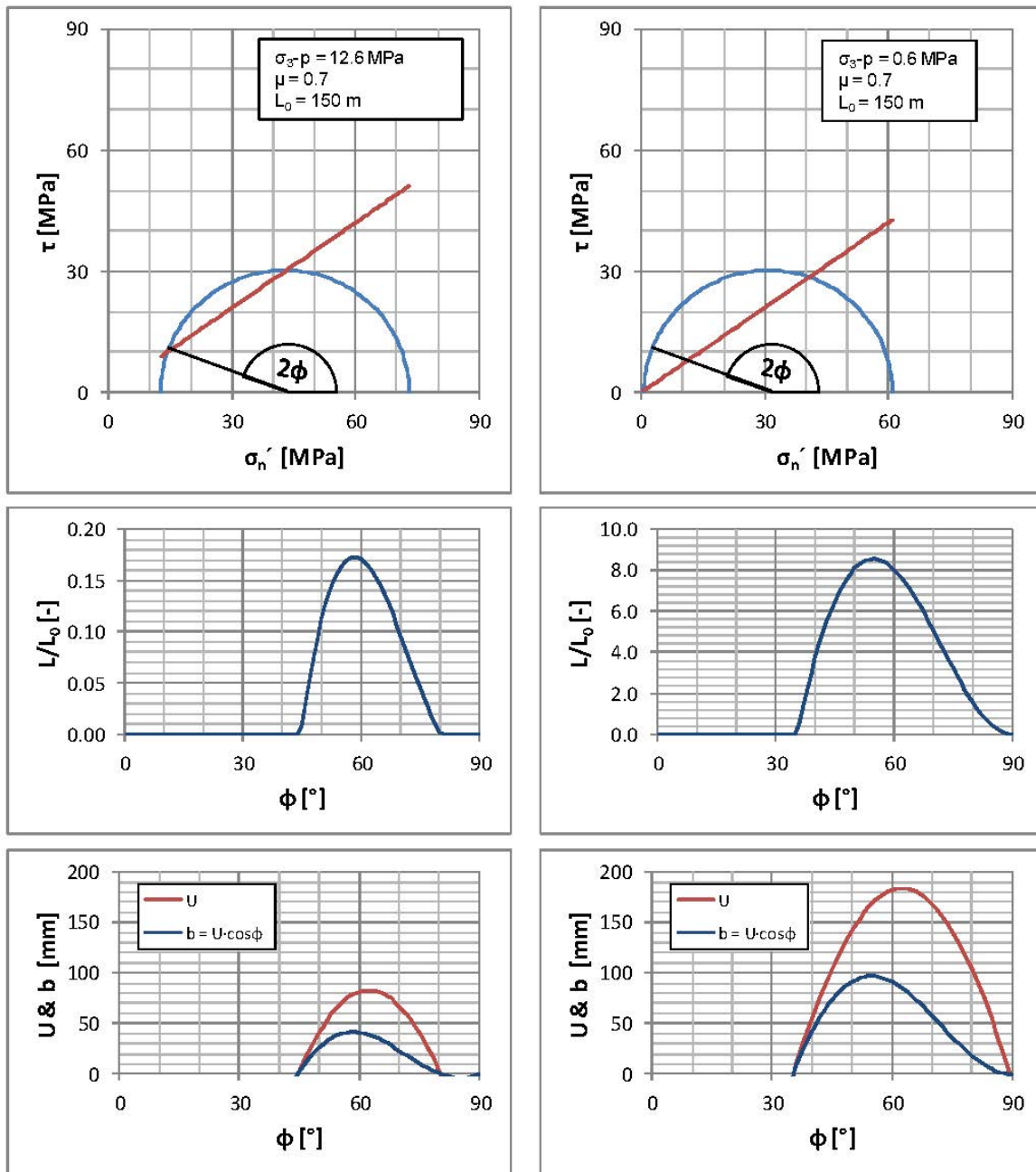
Figure 16. Calculated diagrams for the start of wing-crack propagation (left) and for the end of stimulation (right) in Basel, top: Mohr-diagram ($\sigma_1 = 130$ MPa, $\sigma_3 = 69.6$ MPa at 4600 m depth), middle: normalized wing length L/L_0, bottom: shear displacement U and aperture b at the root of the wings, calculations with equations (6-8), stress data with minor modifications from [30], $\Phi = 80°$.

5. Summary and way forward

Observations and results of all major EGS-projects leave no doubt, that hydraulic stimulation can not be regarded as merely a pressure diffusion process accompanied by shearing and

widening of the joint network. The data rather suggest that generally only one large fracture is formed during massive stimulation tests regardless of the length of the test interval. The formation of these single fractures can well be explained by the wing-crack model. Wing-cracks have a significantly smaller area to volume ratio than tensile fractures of equal size and need therefore larger fluid volumes for an envisaged fracture area. The large shear displacement at the wing roots enables high magnitude seismic events during the propagation period and strong seismic after-shocks by back-sliding. The magnitudes seem to increase with the seismic area and may finally set a limit for the dimensioning of the individual wing-cracks. The post-stimulation transmissibility of wing cracks is presumably very heterogeneous and highly anisotropic. Wide open channels may persist at the roots of the main wings and at the roots of smaller wings within the central shear fracture. These channels are presumably oriented perpendicular to the slip direction and are of uttermost importance for the positioning of the second well to avoid thermal short-circuiting. The transmissibility of the fracture areas in between theses channels and of the large wings is much lower but is most likely in the range of 0.1 - 1 d·m thus enabling flow rates in the order of 1 to more than 10 L/s per wing-crack.

Theses findings suggest that the present EGS-concept will never lead to EGS-systems of industrial size and performance. It has to be abandoned and be replaced by a multi-fracture scheme as foreseen in the original Hot-Dry-Rock concept with the main difference that the tensile fractures of this concept have to be replaced by wing-cracks. This requires a more sophisticated design and planning in particular for the positioning, completion and treatment of the second well. Industrial systems of this type require wells being drilled parallel to the axis of the minimum principal stress, i.e. horizontal wells for normal and strike slip stress conditions and vertical wells for reverse faulting stress conditions. An industrial system may consist of about 30 to 40 equidistant fractures connecting two 1km long parallel well sections with a well separation of about 500 m. Systems of these dimensions should operate for at least 25 years at flow rates of 100 L/s, an electric power output between 5 and 10 MW and a pumping power of less than 1 MW. Directional drilling and packer technology have improved signifi-cantly during the last three decades and multi-fracture concepts are applied with great success in unconventional gas reservoirs. Though the conditions and requirements in geothermal applications are more demanding in various aspects it seems almost certain that geothermal multi-fracture-systems of this type can be realized in the near future.

Author details

Reinhard Jung[*]

Address all correspondence to: jung.geotherm@googlemail.com

Jung-Geotherm, Isernhagen, Germany

References

[1] Smith, M. C, Aamodt, R. L, Potter, R. M, & Brown, D. W. Manmade geothermal reservoirs: Proc. 2nd US Symposium on Geothermal Energy, (1975). San Francisco California, , 1781-1787.

[2] Tester, J. W, Brown, D. W, & Potter, R. M. Hot Dry Rock Geothermal Energy- A new Energy Agenda for the 21st Century. Los Alamos National Lab. Report MS (1989). (LA-11514), 11514.

[3] Duchane, D, & Brown, D. Hot Dry Rock (HDR) geothermal energy research and development at Fenton Hill, New Mexico. GHC Bulletin (2002). , 12-19.

[4] Duchane, D. Hot Dry Rock: A realistic energy option. Geothermal Resources Council Bulletin, March (1990).

[5] Batchelor, A. S. The creation of Hot Dry Rock systems by combined explosive and hydraulic fracturing. In: proceedings of the International Conference on Geothermal Energy, May 1982. Florence, Italy. BHRA Fluid Eng. Bedford; (1982). , 321-342.

[6] Cornet, F. H. Experimental investigations of forced fluid flow through a granite rock mass. In: Proceedings of 4th Int. Seminar on the results of EC Geothermal Energy Demonstration, Florence, Italy, April 27-30, (1989). , 189-204.

[7] Evans, K. F, Zappone, A, Kraft, T, Deichmann, N, & Moia, F. A survey of the induced seismic responses to fluid injection in geothermal and CO2 reservoirs in Europe, doi:j.geothermics.(2011). in Press.

[8] Murphy, H. Hot Dry Rock phase II reservoir engineering. Los Alamos Nat. Lab. Rep. LA-UR-85-3334, (1985).

[9] MIT The Future of Geothermal Energy- Impact of Enhanced Geothermal systems (EGS) on the United States in the 21st CenturyIdaho Nat. Lab., Idaho US, http://geothermal.inel.gov.(2006).

[10] Laney, R, Laughlin, A. W, & Aldrich, M. J. Geology and geochemistry of samples from the Los Alamos National Laboratory HDR Well EE-2, Fenton Hill, New Mexico. Los Alamos Scientific Lab., Los Alamos NM, USA; (1981).

[11] Rowley, J. C, Pettitt, R. A, Matsunaga, I, Dreesen, D. S, Nicholson, R. W, & Sinclair, A. R. Hot-Dry-Rock Geothermal reservoir fracturing initial field operations- (1982). Proceedings Geothermal Resources Council 1983 Annual Meeting, Oct. Portland, Oregon US; 1983., 24-27.

[12] Dreesen, D. S, & Nicholson, R. W. Well completion and operations for the MHF of Fenton Hill HDR Well EE-2. Proceedings Geothermal Resources Council, Kailua-Kona, Hawaii, Aug. (1985). , 26-30.

[13] Parker, R. H. Overview. In: Parker R.H. ed., Hot Dry Rock geothermal energy, Phase 2B final report of the Camborne School of Mines Project, (1989). , 1, 3-38.

[14] Baria, R, Green, A. S. P, & Hearn, K. C. Microseismic results. In: Parker R.H. ed., Hot Dry Rock geothermal energy, Phase 2B final report of the Camborne School of Mines Project., (1989). , 2, 682-740.

[15] Kappelmeyer, O, Gerard, A, Schloemer, W, Ferrandes, R, Rummel, F, & Benderitter, Y. European HDR Project at Soultz-sous-Forêts: General presentation. In: Geothermal Energy in Europe, J.C. Bresee ed., Gordon and Breach Science Publ., (1992).

[16] Sausse, J, & Genter, A. Types of permeable fractures in granite.- Geological Soc., London, Special Publications (2005). doi:10.1144/GLS.SP.2005.240.01.01., 240, 1-14.

[17] Cornet, F. H, Bérard, F. H, & Bourouis, S. How close to failure is a granite rock mass at 5 km depth?. International Journal Rock Mechanics Mining Sciences (2007). , 47-66.

[18] Klee, G, & Rummel, F. Hydrofrac stress data for the European HDR research project test site Soultz-sous-Forêts. International Journal of Rock Mechanics, Mining Science and Geomechanics Abstracts (1993). , 973-976.

[19] Jung, R. Hydraulic fracturing and hydraulic testing in the granitic section of borehole GPK1, Soultz Sous Forêts. Geotherm. Sci. & Tech. (1991). , 3, 149-198.

[20] Jung, R. HDR-Projekt Soultz- Erschließung permeabler Risszonen für die Gewinnung geothermischer Energie aus heißen Tiefengesteinen. Schlussbericht zum Forschungsvorhaben 0326690A, Archiv Nr. 118977, Bundesanstalt für Geowissenschaften und Rohstoffe, Hannover, (1999).

[21] Baria, R, Jung, R, Tischner, T, Teza, D, Baumgärtner, J, Dyer, B, Hettkamp, T, Nicholls, J, Michelet, S, Sanjuan, B, Soma, N, Asanuma, H, & Garnish, J. Creation of a HDR/EGS reservoir at 5000 m depth at the European HDR project.- Proc. 31st Stanford Geothermal Workshop (2006). Stanford, Cal., US.

[22] Weidler, R. Personal Communication, Geothermeon, Landau, Germany, (2001).

[23] Jung, R. Hydraulic in situ investigations of an artificial fracture in the Falkenberg Granite. Int. J. Rock Mech. Sci. & Geomech. Abstr.; (1989). , 26(3), 301-308.

[24] Murphy, H, Keppler, H, & Dash, Z. Does hydraulic fracturing theory work in jointed rock masses?- Geothermal Resources Council, Transactions Oct. (1983). , 7, 461-466.

[25] Camborne School of MinesGeothermal Energy Project. Internal report (1985). , 2-42.

[26] Nedo, F. Y. Summary of Hot Dry Rock Geothermal Power Project. Geothermal Energy Technology Dep., New Energy and Ind. Tech. Dev. Org., Tsukuba, Japan; (1997).

[27] Tezuka, K, & Niitsuma, H. Stress estimated using microseismic clusters and its relationship to the fracture system of the Hijiori hot dry rock reservoir, Eng. Geol. 56; (2000). , 47-62.

[28] Kaieda, H, Hisatoshi, I, Kenzo, K, Koichi, S, Hiroshi, S, & Koichi, S. Review of Ogachi HDR Project in Japan. Proc. IGA World Geotherm. Congress 2005, Antalya Turkey, April 2005; (2005). , 24-29.

[29] Jones, R, Beauce, A, Fabriol, H, & Dyers, B. Imaging induced microseismicity during the 1993 injection test at Soultz-sous-Forêts France, Proc. IGA World Geothermal Congress, Florence, Italy; (1995).

[30] Häring, M. O, Schanz, U, Ladner, F, & Dyer, B. C. Characterization of the Basel1 Enhanced Geothermal System. Geothermics; (2008). doi:10.1016/j.geothermics. 2008.06.002.

[31] Evans, K. F, Moriya, H, Niitsuma, H, Jones, R. H, Phillips, W. S, Genter, A, Sausse, J, Jung, R, & Baria, R. Microseismicity and permeability enhancement of hydro-geologic structures during massive fluid injections into granite at 3 km depth at the Soultz HDR site. Geophys. J. Int., (2005). , 2005(160), 388-412.

[32] Niitsuma, H, Asanuma, H & Jones, R. Induced seismicity, AP 3000 report. In: Baisch, S. (ed.) Deep Heat Mining Basel – Seismic Risk Analysis. Basel, Amt für Umwelt und Energie; (2009). AP 3000 p1-62.

[33] Tischner, T, Pfender, M, & Teza, D. Hot Dry Rock Projekt Soultz: Erste Phase der Erstellung einer wissenschaftlichen Pilotanlage. Abschlussbericht zum Vorhaben 0327097, Bundesministerium für Umwelt, Naturschutz und Reaktorsicherheit, 1.4.Berlin, Germany; (2006). , 2001-31.

[34] Ledingham, P. Circulation results 1983-1986, 7:2 Thermal Model. In: Parker R.H. ed., Hot Dry Rock geothermal energy, Phase 2B final report of the Camborne School of Mines Project., (1989). , 1, 390-408.

[35] Matsunaga, I, Yanagisawa, N, Sugita, H, & Tao, H. Reservoir monitoring by tracer testing during a long term circulation test at the Hijiori HDR Site. Proc. 27th Workshop on Geothermal Reservoir Eng., Stanford Univ. Stanford, Jan. (2002). , 28-30.

[36] Tenma, N, Yamaguchi, T, Tezuka, K, Oikawa, Y, & Zyvolovski, G. Comparision of heat extraction from production wells in the shallow and deep reservoirs at the Hijiori test site using FEHM code. Proc. 26. Workshop on Geothermal Reservoir Engineering, Stanford Uni., January February 1, 2001, SGP-TR-162; (2001). , 29.

[37] Matsunaga, I, Sugita, H, & Tao, H. Tracer monitoring by a fibre optic fluorometer during a long-term circulation test at the Hijiori HDR Site. Proc. 26. Workshop on Geothermal Reservoir Eng., Stanford Univ. Stanford, Jan. (2001). , 29-31.

[38] Oikawa, Y, Tenma, N, Yamaguchi, T, Karasawa, H, Egawa, Y, & Yamauchi, T. Heat extraction experiment at Hijiori Test Site. Proc. 26. Workshop on Geothermal Reservoir Eng., Stanford Univ. Stanford, Jan. (2001). , 29-31.

[39] Kenzo, K. Technology of reservoir estimation for Hot Dry Rock geothermal power. Volumetric Estimation of the Ogachi Reservoir by Tracer Test. Denryoku Chuo Kenkyujo Abiko Kenkyujo Hokoku, (2000). p.(U99018)

[40] Genter, A, Dezayes, C, & Gentier, S. Lede´sert B., Sausse´ J. Conceptual fracture model at Soultz based on geological data. In: Bundesanstalt für Geowissenschaften und Rohstoffe und den staatlichen Geologischen Diensten in der Bundesrepublik Deutschland (eds.) International Conference 4th HDR Forum, 29-30 Sep. 1998, Strasbourg, France. Geologisches Jahrbuch, Sonderhefte, Heft SE1, Reihe E, Geophysik, (2002). , 93-102.

[41] Valley, B. C. The relation between natural fracturing and stress heterogeneities in deep-seated crystalline rocks at Soultz-sous-Forêts (France), PhD thesis. ETH Zürich, (2007). (17385)

[42] Cotterell, B, & Rice, J. R. International Journal of Fracture 16; (1980). , 155-169.

[43] Lehner, F, & Kachanov, M. On modelling of "winged" cracks forming under compression. International Journal of Fracture 77; (1996). RR75., 69.

[44] Baisch, S, & Vörös, R. Personal Communication. Q-Con, Bad Bergzabern, Germany; (2007).